Experimental Study of Low-yield Strength Steel Buckling Restrained Brace

N. Ma & J.P. Ou
Dalian University of Technology, China
H. Li
Harbin Institute of Technology, China

SUMMARY:
All-steel buckling-restrained braces (BRBs) produced by common building steels can not control the damage of reinforced concrete structures with small ductility. Low-yield strength steel presents plasticity under small strain, which is expected to fabricate all-steel BRBs with better ductility and energy dissipation capacity. In this study, the mechanical properties of Q100, a novel low-yield strength steel developed in China, were tested by quasi-static tension experiments. The results indicated that Q100 presented low yield strength ~100MPa under the tensile strain of ~0.05%. It was used to fabricate the core plates for two all-steel BRBs, the outer tubes of which were made of Q235. Component test was conducted under uniaxial increasing-amplitude quasi-static cyclic loading, the maximum strain amplitude of which was 3%. The two all-steel low-yield strength BRBs presented rich hysteretic loops. The cumulative inelastic ductility factors of the two braces were 841 and 1238, respectively. Their strain hardening coefficients and combined strength promotion coefficients were larger than those of the BRBs made by common building steels. The results indicated that the low-yield strength BRBs present outstanding ductility and energy dissipation capacity, and they can be used in reinforced concrete frames as well as the structures need to suffer strong wind.

Keywords: Buckling-restrained brace, low-yield strength steel, ductility, energy dissipation capacity

1. INTRODUCTION

The idea of using damping devices in a building frame to absorb large portions of the seismic energy has become popular in damage control design for civil structures since 1975 (Kelly et al). During an earthquake, damping devices are expected to present plasticity prior to the main structure; hence, the damage of the main structure can be controlled (Dargush et al. 1995). As one kind of the damping devices, buckling-restrained braces (BRBs) offers strength and energy dissipation while at the same time showing well-distributed yielding, and attracted more and more attentions (Mirtaheri et al. 2011; Kim et al. 2006; Usami et al. 2005).

The concept of BRB was first proposed by Kimura *et al*. Over the last few decades, a significant amount of research works have been performed in Japan, USA, and China (Xie 2005; Takeuchi et al. 2010; Marshall et al. 2010; Ma et al.2008; Chou et al. 2010). A detailed summary of those works were summarized by Uang *et al*. A typical BRB consists of a core segment and a buckling restraining member; the former carries the axial load, while the later provides lateral support to the core and prevents it from buckling in compression at the target lateral displacement (Watanabe et al. 1988). According to the restraining mechanism, BRBs can be grouped into two main categories: one is restrained by a concrete or mortar filled steel encasing member (Black et al. 2004), and the other one is inhibited by all-steel sections, *i.e.* all-steel BRB. Compared with the BRBs restrained by filling steel components, all-steel BRBs exhibit such advantages as lighter weight, easier fabrication and easier quality control.

The core plate for an all-steel BRB was usually fabricated with common building steels, just like its restrained member. For example, Q235, the nominal yield strength of which is 235MPa, were widely used to produce core plates in China. For the steel frames with large ductility, those common building steels with large yield strength are suitable materials to make the core plates. However, for the reinforced concrete frames with small ductility, in which BRBs are required to exhibit plasticity at small displacement, the common building steels can not meet the need. Besides, the all-steel BRB with a core plate made by common steels only can be used to control the damage of the main structure under moderate or severe seismic; when the structure is subjected to a minor seismic or strong wind, the BRB will not work. To overcome those shortcomings, the idea of using the steel with low-yield strength to fabricate the core plate has been proposed. Several works have been done in Japan and Taiwan (Saekei et al. 1995; Susantha et al. 2005), the results of which indicate the BRBs with core plates made by low-yield strength present good energy dispassion properties under low stress (Maeda et al. 1998; Matteis et al. 2003). Nevertheless, the maximum axial strain amplitude in most studies was 1.5%, which did not give full play to the good ductility of the low-yield strength steels. In this study, the properties of all-steel BRBs with core plates made by steel Q100, the nominal yield strength of which is 100MPa, will be evaluated by component test at large deformation.

2. MECHANICAL PROPERTIES OF LOW-YIELD STRENGTH STEEL

Q100 steel with nominal yield strength of 100MPa, provided by Anshan Steel Group, China, was adopted as the low-yield strength to fabricate the core plate of all-steel BRBs. Considering it is a novel material, its composition was analyzed by X-ray Diffraction, and the results are listed in Table 2.1. The content of carbon is only 0.014%, which is much lower than that in structural low carbon steel Q235, in which the carbon content is in the range between 0.14% and 0.22%.

Table. 2.1. The composition of Q100

Element	C	Si	Mn	S	P
Content（%）	0.014	＜0.01	0.19	0.0046	0.012

To examine the mechanical properties of the low-yield strength steel, three tensile samples with rectangular cross section were fabricated and tested under quasi-static loading. The loading speed was 312.5 με/s. The dependence of the tensile stress on tensile strain for all the samples was shown in Fig. 2.1, the inset figure is the partial enlarged detail in the tensile strain range between 0% and 1%. It indicates the Q100 steel has an obvious yield point, the tensile strain at which is ~0.05%. The detailed mechanical properties are listed in Table 2.2. All the three samples presented similar mechanical properties. Their average yield strength and average elongation at break was 90.3MPa and 60%, respectively. It indicates the Q100 steel has stable and outstanding ductility, which make it have the potential to be used in all-steel BRBs to control the damage of reinforced concrete structures or structures that subjected to strong wind.

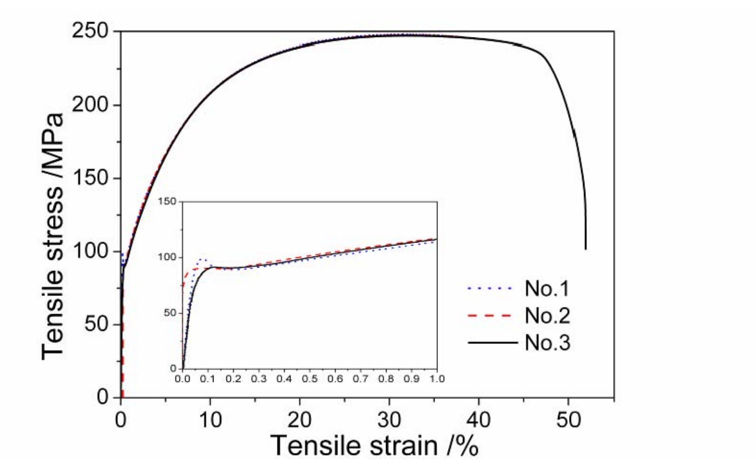

Figure 2.1. Relationships between tensile stress and tensile strain of three Q100 steel samples

Table 2.2. Quasi-static tensile properties of Q100 steel

No.	Yield strength (MPa)	Tensile strength (MPa)	Young's modulus (MPa)	Elongation at break (%)
No.1	91	247	1.62×10^5	58.5
No.2	90	247.4	1.87×10^5	60.2
No.3	90	248	2×10^5	61.4
Average	90.3	247.5	1.83×10^5	60

3. DESIGN OF ALL-STEEL BRB SPECIMENS

The core plate of the all-steel BRB specimens were made by Q100 steel, while the outer tube were fabricated with structural steel Q235, the nominal yield strength of which is 235MPa. The design strain of the BRB was 3%, which was corresponding to 1/5000 story drift of a reinforced concrete frame.

As shown in Fig.3.1, the cross section of the core plate of the BRB is rectangular. The core plate connects with the two gusset plates by bolting with connection plates, which are formed by two pieces of steel angle. To ensure the two ends of the core plate in elastic state, their width is enlarged. The outer tube is formed by welding four pieces of unequal steel angle and two pieces of steel plate. The multi-wave deformation of the core plate under compression is restrained by the unequal steel angle, which prevents the local buckling from occurrence. The two pieces of restraining steel plate are used to prevent the core plate from bending over the width direction under large deformation. Besides, to prevent the out-of-plane rotation at the ends of the core plate where is no constraint, a rotation restraint composed by four quarter restraint members is setup at each end. One side of the quarter restraint is welded with the connection plate, while the other side is lapped with the outer tube. A stiffening hoop is setup at each end of the outer tube to ensure the cooperation of the four pieces of unequal steel angle as well as to keep the tube from damage under shear stress. Two specimens were fabricated with the same configuration, which were named as BRB-1 and BRB-2, respectively.

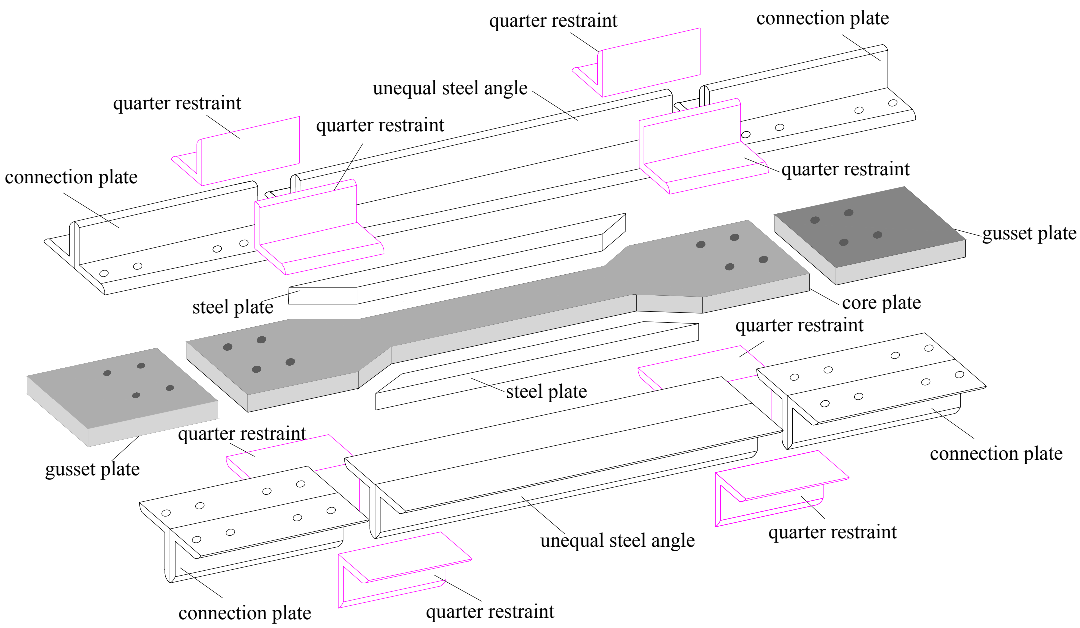

Figure 3.1. Configuration of BRB specimen

The gap between the core plate and the outer tube is a key parameter that influences the energy dissipation capacity of the all-steel BRB. In ideal case, the gap is designed to make itself be 0 mm when the brace suffer the maximum designed deformation. However, in practical case, the machining accuracy has to be considered. Therefore, the gap is designed to be a little larger than the ideal value; the gap between the core plate and the steel angle is 1 mm, while the gap between the core plate and the steel plate is 2 mm. To prevent the outer tube from slipping down when the core is under the axial force, the sloped edge of the restraining steel plate is fabricated to match the transition portion of the core plate.

The parameters of the specimens are summarized in Table 3.1, where L and L_y represent the length of the whole core plate and the length of the yielding portion of the core plate, respectively. A_y represents the cross section area of the core plate in yield portion, and A_1 represents the cross section area of the core plate at the end portion. b and t is the width and the thickness of the core plate, respectively. P_e represents Euler critical load of the outer tube, and P_y is the yielding force of the core plate. δ_1 is the gap between the core plate and the angle steel, and δ_2 represents the gap between the core plate and the restraining steel plate.

Table 3.1. Parameters of the specimens

L(mm)	L_y(mm)	b(mm)	t(mm)	A_y(mm^2)	δ_1(mm)	δ_2(mm)	A_1/A_y	b/t	P_e/P_y
1186	616	86	15	1290	1	2	2.6	5.7	18

4. COMPONENT TEST

4.1. Test setup

The component test was conducted at the Structural and Seismic Testing Center, Harbin Institute of Technology. Uniaxial quasi-static cyclic loading was applied by the MTS electro-hydraulic testing machine with a capacity of 2500 kN. The axial force of the specimens was measured by the loading cell of the MTS actuator. To measure the axial deformation of the core plate accurately, two string potentiometers (SP-1 and SP-2) were mounted between the two enlarged end plates. The mounting positions are close to the yield portion of the core plate. To measure the brace ends rotation, four displacement transducers (named LVDT-1 to LVDT-4) were set on a metal support fixed on the ground. Two mounting positions were on the upper enlarged end of the core plate, while the other two were on the lower enlarged end of the core plate. The test setup is shown in Fig. 4.1.

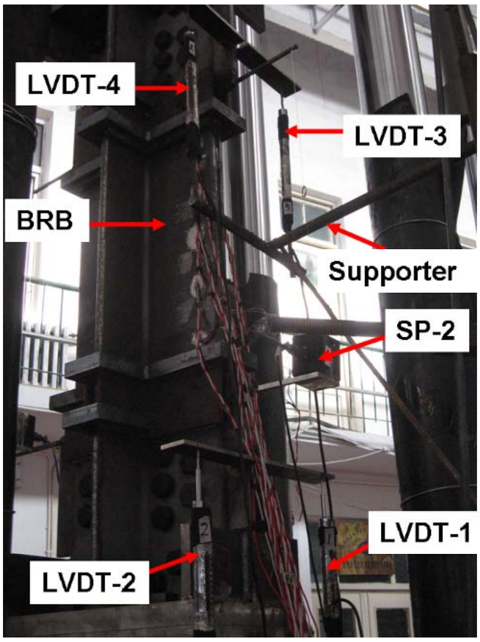

Figure 4.1. Photo of component test setup

4.2. Loading protocol

The two specimens were subjected to an increasing-amplitude quasi-static cyclic loading under deformation-control method, as shown in Table 4.1. The loading speed was a constant, 0.1925 mm/s, which was consistent with that in the material test, *i.e.* 312.5 με/s. Each loading cycle was started with tension. For the first three loading grades (loading amplitude corresponds to the core strain of 0.5%, 1% and 2%, respectively), the number of loading cycle was 3. When the three loading grades were finished, the cyclic loading was imposed at the design core strain amplitude of 3% until the brace failed with declined load-bearing capacity.

Table 4.1. Loading protocol

Loading grade	Target strain (%)	Target control displacement (mm)	Number of cycles
1	0.5%	3.3	3
2	1%	6.6	3
3	2%	13.3	3
4	3%	20	to failure

4.3. Results and discussion

BRB-1 performed well in the first three loading grades. Under the fourth loading grade, the loading amplitude of which was 3%, the brace exhibited slight decline of bearing capacity at the maximum tensile strain in the fourth cycle, but it still could bear loading. However, at the maximum tensile strain in the fifth cycle, the bearing capacity dropped dramatically, which indicated the tensile rapture of the core plate. The specimen shows rich hysteretic loops, as shown in Fig. 4.2. It indicated the brace had stable energy absorption capacity. After the test, the specimen was taken apart to examine its failure mode. As shown in Fig. 4.3, the core plate showed fracture at the position near one end of the core. The possible reason for the failure mode is that there was some flaw in the material.

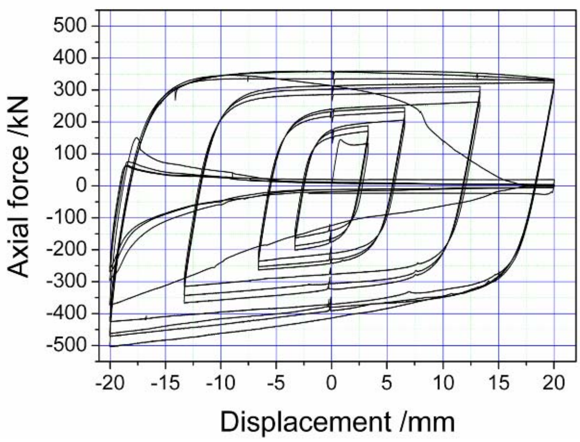

Figure 4.2. Hysteretic curves of BRB-1

BRB-2 performed well in the first three loading grades and in the first 6 cycles at the fourth loading grade, the strain amplitude of which was 3%. During the tension at the seventh loading cycle, the bearing capacity of the brace declined to 30kN dramatically. However, no obvious buckling or other forms of failure were observed on the outer tube, as shown in Fig. 4.4. Then the specimen was taken apart to examine its failure mode. As shown in Fig. 4.5, BRB-2 also failed in tensile failure, the failure pattern was similar with that of BRB-1. Due to the strict constraint by the outer tube, the amplitude of the buckling wave of the core plate was small, as shown in Fig.4.6.

Figure 4.3. Failure mode of BRB-1

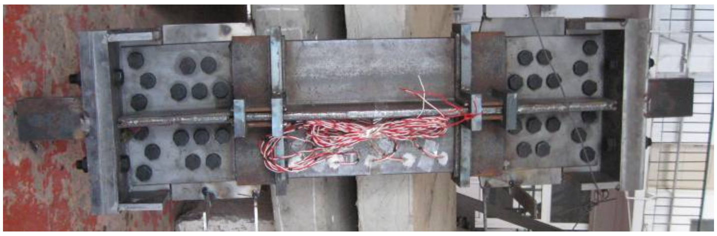

Figure 4.4. View of BRB-2 after component test

Figure 4.5. Failure mode of BRB-2

Figure 4.6. Multi-wave buckling of the core plate of BRB-2

Figure 4.7 shows the hysteretic curves of BRB-2. As it is shown, BRB-2 presents rich hysteretic loops, and obvious cycle hardening phenomenon is observed. The maximum compression force of the fourth cycle at the loading amplitude of 3% is larger than those of the previous three cycles at the same loading amplitude; the maximum compression force of the sixth cycle is much larger than the previous cycles. The reason is possibly that the outer tube bulged in some positions with increasing loading cycles, which made the gap between the core plate and the outer tube become increasingly larger, as a result, the fiction force between the two parts increased.

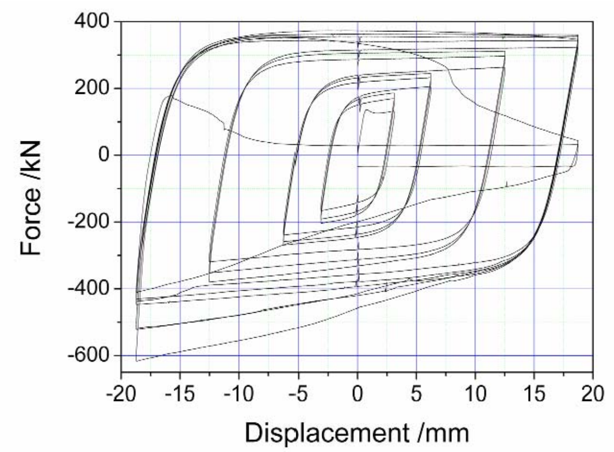

Figure 4.7. Hysteretic curves of BRB-2

Several parameters are used to evaluate the properties of the low-yield strength steel BRBs. Strain hardening coefficient ω_i is defined by the ratio of the maximum tensile stress to the yield stress in the ith loading cycle. The maximum ductility in the ith loading cycle μ_{max} is defined by the ratio of the maximum deformation to the yield deformation, while the sum of μ_{max} of all the loading cycles is defined as cumulative inelastic ductility factor. Compression strength adjustment factor β_i is defined by the ratio of the maximum compression force to the maximum tension force in the ith loading cycle, which reflects the influence of the friction force between the core plate and the outer tube and the Poisson's effect of the core plate under compression on properties of the BRBs. All of those parameters are listed in Table 4.2. The strain hardening coefficient ω_i increases with increasing loading cycle number; for the two braces, ω_i approaches or exceeds 3 at the loading amplitude of 3%, which is larger than that of the all-steel BRB with a core plate made by Q235. It indicates the low-yield strength BRB presents more significant strain hardening effect. For the two braces, their compression strength adjustment factor β_i in majority cycles is less than 1.3. In the last few cycles, β_i is a little larger than 1.3, one reason was the tensile stress declined due to the emergence of cracks in the core plate, and another reason was the compression stress increased with increasing friction force between the core plate and the outer tube. The maximum combined strength promotion coefficient $\omega_i\beta_i$ is 5. It indicates the low-yield strength BRB not only presents lower yield force, but also shows larger bearing capacity, which should be taken into consideration in the design of frames, gusset plates and BRBs. The cumulative inelastic ductility factors of BRB-1 and BRB-2 are 841 and 1238, respectively. They are much larger than the requirement of 200 in the SEAOC-AISC Recommended Provisions as well as the value of the BRBs fabricated with Q235. It indicates the low-yield strength BRB presents outstanding ductility and energy dissipation capacity.

Table 4.2. Parameters for evaluation of the properties of the two BRBs

Specimen	Loading amplitude	Serial number	ω_i	β_i	$\omega_i\beta_i$	ε_{max}	μ_{max}	$\sum\mu$
BRB-1	0.5%	1	0.8	1.47	1.19	3%	30	841
		2	1.26	1.10	1.38			
		3	1.38	1.07	1.48			
	1%	4	1.51	1.15	1.74			
		5	1.71	1.09	1.86			
		6	1.70	1.07	1.93			
	2%	7	1.93	1.13	2.17			
		8	2.03	1.24	2.52			
		9	2.29	1.18	2.71			
	3%	10	2.38	1.31	3.12			
		11	2.46	1.41	3.46			
		12	2.64	1.28	3.39			
		13	2.65	1.39	3.70			
BRB-2	0.5%	1	1.08	1.25	1.35	3%	34	1238
		2	1.39	1.12	1.56			
		3	1.52	1.09	1.66			
	1%	4	1.68	1.16	1.95			
		5	1.89	1.12	2.11			
		6	2	1.09	2.19			
	2%	7	2.15	1.22	2.61			
		8	2.43	1.19	2.89			
		9	2.55	1.22	3.11			
	3%	10	2.65	1.35	3.58			
		11	2.81	1.26	3.53			
		12	2.90	1.26	3.66			
		13	2.98	1.43	4.25			
		14	2.96	1.44	4.26			
		15	3.06	1.65	5.05			

5. CONCLUSION

A novel low-yield strength steel Q100 with the yield strength of 100 MPa was used to fabricate all-steel BRBs. The properties of two braces were experimentally studied by component test using MTS. Increasing-amplitude quasi-static cyclic loading protocol was applied on the specimens. The two braces presented rich hysteretic loops, obvious cycle hardening phenomenon, large strain hardening coefficient, and large combined strength promotion coefficient. The cumulative inelastic ductility factors of two braces were 841 and 1238, respectively, which were much larger than the requirement of 200 in the SEAOC-AISC Recommended Provisions. In conclusion, the low-yield strength BRB presents better ductility and larger energy dissipation capacity than the BRBs made by common building steels, which make it can be used to control the damage of reinforced concrete frames with low ductility and the structures subjected to minor seismic or strong wind.

ACKNOWLEDGEMENTS
This research is financial funded by the National Natural Science Foundation of China under the grant number of 51108063, and the China Postdoctoral Science Foundation under the Grant number of 20110491536.

REFERENCES

Black, C., Makris, N. and Aiken, I. (2004). Component testing, seismic evaluation and characterization of buckling-restrained braces. *Journal of Structural Engineering* **130**:6, 880-894

Choi, H., Kim, J. and Chung, L. (2006). Seismic design of buckling-restrained braced frames based on a modified energy-balance concept. *Canadian Jounral of Civil Engineering* **33**:1251-1260

Chou, C. and Chen, S. (2010). Subassemblage tests and finite element analyses of sandwiched buckling restrained braces. *Engineering Structures* **32**:2108-2121.

Dargush, G. F. and Soong, T. T. (1995). Behavior of metallic plate dampers in seismic passive energy dissipation systems. *Earthquake Spectra* **11**:4, 545-568

Kelly, J. M., Skinner, R. I. and Heine, A. J. (1972). Mechanisms of energy absorption in special devices for use in earthquake resistant structures. *Bulletin of N.Z. Society for Earthquake Engineering* **5**:3, 63-88

Kim, J. and Choi, H. (2004). Behavior and design of structures with buckling-restrained braces. *Engineering Structures* **26**: 693-706

Ma, N., Wu, B., Zhao, J. X., Li, H., Ou, J. P. and Yang, W. B. Full scale test of all-steel buckling restrained braces. *Proceeding of the 14th World Conference on Earthquake Engineering*

Maeda, Y., Nakata, Y. and Iwata, M. (1998). Fatigue properties of axial yield type hysteresis dampers. *J. Struct. Constr. Eng.* **503**:109-115

Marshall, J. D. and Charney, F.A. (2010). A hybrid passive control device for steel structures, Ⅰ: development and analysis. *Journal of Constructional Steel Research* **66**:1278-1286

Matteis, G. D., Landolfo, R. and Mazzolani, F.M. (2003). Seismic response of MR steel frames with low-yield steel shear panels. *Engineering Structures* **25**:155-168

Mirtaheri, M., Gheidi, A. and Zandi, A. (2011). Experimental optimization studies on steel core lengths in buckling restrained braces. *Journal of Constructional Steel Research* **67**:1244-1253

Saeki, E., Sugisawa, M. and Yamaguchi, T. (1995). A study on hysteresis and hysteresis energy characteristics of low yield strength steel. *J. Struct. Constr. Eng.* **473**:159-168

Saeki, E., Sugisawa, M. and Yamaguchi, T. (1995). A study on low cycle fatigue characteristics of low yield strength steel. *J. Struct. Constr. Eng.* **472**:139-147

Skinner, R. I., Kelly, M. J. and Heine, A. J. (1975). Hysteretic dampers for earthquake-resistant structures. *Earthquake Engineering and Structural Dynamics* **3**: 287-296.

Spencer, B. F. J. and Nagarajaiah, S. (2003). State of the art of structural control. *Journal of Structural Engineering* **129:7**, 845-856

Susantha, K.A.S., Aokia, T. and Kumano, T. (2005). Applicability of low-yield-strength steel for ductility improvement of steel bridge piers. *Engineering Structures* **27**:1064-1073

Takeuchi, T., Hajjar, J. F. and Matsui, R. (2010). Local buckling restraint condition for core plates in buckling restrained braces. *Journal of Constructional Steel Research* **66**(2):139-149

Uang, C. M., Nakashima, M. and Tsai, K. C. (2004). Research and application of buckling-restrained braced frames. *International Journal of Steel Structures* **4**:301-313

Usami, T., Lu, Z. and Ge, H. (2005). A seismic upgrading method for steel arch bridges using buckling restrained brace. *Earthquake Engineering and Structural Dynamics* **34**:471-496

Watanabe, A., Hitomi, Y. and Yaeki, E. (1988). Properties of brace encased in buckling-restraining concrete and steel tube. *Proceedings of the 9th World Conference on Earthquake Engineering* **9**:719-724

Xie, Q. (2005). State of the art of buckling-restrained braces in Asia. *Journal of Constructional Steel Research* **61**:727-748